

This is a provisional PDF only. Copyedited and fully formatted version will be made available soon.

Folia Histochemica et Cytobiologica

ISSN: 0239-8508

e-ISSN: 1897-5631

Mitofusin 2 inhibits high glucose-induced apoptosis of human lens epithelial cells via modulating mitochondrial function and autophagy

Authors: Yuan-Yi Guo, Jiang-Yue Zhao, Han-Rong Li, Zhuo Guo, Hao-Yue Shen

DOI: 10.5603/fhc.98875

Article type: Original paper

Submitted: 2024-01-10

Accepted: 2024-06-03

Published online: 2024-06-19

This article has been peer reviewed and published immediately upon acceptance. It is an open access article, which means that it can be downloaded, printed, and distributed freely, provided the work is properly cited.

Articles in "Folia Histochemica et Cytobiologica" are listed in PubMed.
Pre-print author's version.

ORIGINAL PAPER

Mitofusin 2 inhibits high glucose-induced apoptosis of human lens epithelial cells via modulating mitochondrial function and autophagy

Yuan-Yi Guo¹, Jiang-Yue Zhao², Han-Rong Li², Zhuo Guo², Hao-Yue Shen²

¹Department of Ophthalmology, the Fourth People's Hospital of Shenyang, Shenyang, Liaoning Province, People's Republic of China

²Department of Ophthalmology, the Fourth Affiliated Hospital of China Medical University, Shenyang, Liaoning Province, People's Republic of China

Correspondence addresses:

Dr. Yuan-Yi Guo

Department of Ophthalmology, the Fourth People's Hospital of Shenyang

No. 20, Huanghe South Street, Shenyang, Liaoning Province, People's Republic of China

e-mail: gyy_91zgysy@163.com

Dr. Jiang-Yue Zhao

Department of Ophthalmology, the Fourth Affiliated Hospital of China Medical University,

No. 4, Chongshan East Road, Shenyang, Liaoning Province, People's Republic of China

e-mail: jyzhao@cmu.edu.cn

Abstract

Introduction. Diabetic cataract (DC) is a common ocular complication of diabetes. Mitofusin 2 (MFN2), a mitochondrial fusion protein, is involved in the pathogenesis of cataract and diabetic complications. However, its role and molecular mechanisms in DC remain unclear.

Materials and methods. DC models in rats were induced by intraperitoneal injection of streptozocin (STZ) for 12 weeks. We measured the body weight of rats, blood glucose concentrations, sorbitol dehydrogenase (SDH) activity and advanced glycation end products (AGE) content in the lenses of rats. MFN2 mRNA and protein expression levels in the lenses were detected by RT-qPCR and western blot assays. *In vitro*, human lens epithelial (HLE) B3 cells were treated for 48 h with 25 mM glucose (high glucose, HG) to induce cell damage. To determine the role of MFN2 in HG-induced cell damage, HLE-B3 cells were transfected with lentivirus loaded with MFN2 overexpression plasmid or short hairpin RNA (shRNA) to overexpress or knock down MFN2 expression, followed by HG exposure. Cell viability was assessed by CCK-8 assay. Flow cytometry was used to detect cell apoptosis and reactive oxygen species (ROS) level. JC-1 staining showed the changes in mitochondrial membrane potential ($\Delta\psi_m$). The mediators related to apoptosis, mitochondrial damage, and autophagy were determined.

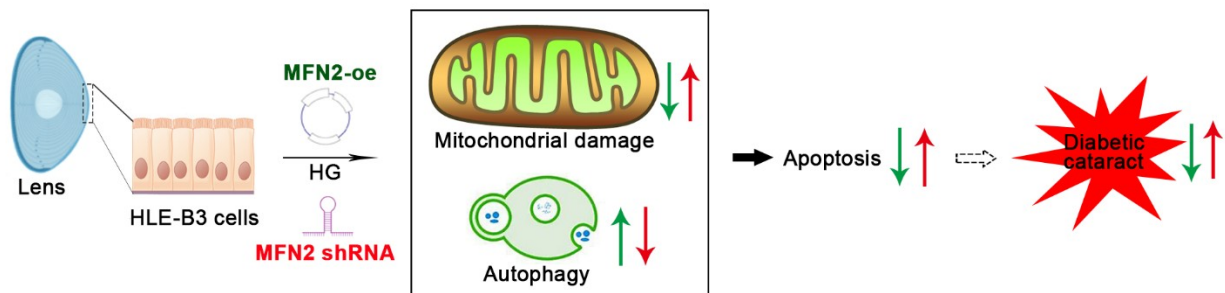
Results. STZ-administrated rats showed reduced body weight, increased blood glucose levels, elevated SDH activity and AGE content, suggesting successful establishment of the DC rat model. Interestingly, MFN2 expression was significantly downregulated in DC rat lens and HG-induced HLE-B3 cells. Further analysis showed that under HG conditions, MFN2 overexpression enhanced cell viability and inhibited apoptosis accompanied by decreased Bax, cleaved caspase-9 and increased Bcl-2 expression in HLE-B3 cells. MFN2 overexpression also suppressed the mitochondrial damage elicited by HG as manifested by reduced ROS production, recovered $\Delta\psi_m$ and increased mitochondrial cytochrome c (Cyto c) level. Moreover, MFN2 overexpression increased LC3BII/LC3BI ratio and Beclin-1 expression, but decreased p62 level, and blocked the phosphorylation of mTOR in HG-treated HLE-B3 cells. In contrast, MFN2 silencing exerted opposite effects.

Conclusions. Our findings indicate that MFN2 expression may be essential for preventing

lens epithelial cell apoptosis during development of diabetic cataract.

Keywords: MFN2; overexpression; diabetic cataract; mitochondrial membrane potential; autophagy; apoptosis

Graphical abstract



Introduction

Diabetes mellitus, a metabolic disease characterized by elevated serum/blood glucose concentration, is expected to afflict 629 million people worldwide by the year 2045 [1]. Diabetic cataract (DC) is a common complication of diabetes, generally defined as lens opacity, and is the leading cause of blindness globally [1, 2]. Abundant evidence indicates that patients with diabetes are accompanied by increased incidence and earlier development of cataracts [3, 4]. At present, surgery has been accepted as the best method to treat cataract, but it possibly increases the risk of diabetes-related complications [4, 5]. Lens epithelial cells (LECs), located in the anterior capsule of the lens, are responsible for the differentiation of lens fiber cells and for maintaining the transparency of the lens [6]. LEC apoptosis is the molecular basis of cataractogenesis [7–9], and the injury of which may contribute to the progression of DC. Therefore, inhibition of LEC apoptosis is of great significance in preventing the development of DC.

Mitochondrial fusion, a major process of mitochondrial dynamics, is found to possess a beneficial role in mitochondrial homeostasis [10]. Mitofusin 2 (MFN2), a conserved mitochondrial fusion protein primarily localized in the outer membrane of mitochondria, however, its expression has also been noted in the cytosol [11]. MFN2 has been reported to be implicated in the regulation of the progression of human obesity and type 2 diabetes [12, 13]. MFN2 attenuates kidney lesion [14, 15] and repairs retinal endothelial cell damage in diabetic rats [14–16]. A study of MFN2 conditional knockout in rat embryo revealed that loss of MFN2 function increased apoptosis and mitochondrial impairment in LECs, thereby leading to congenital eye defects including opacified lens [17]. Interestingly, the expression of MFN2 is widely downregulated in the kidney, heart, penile tissue and retina of streptozotocin (STZ)-induced diabetic rats compared to normal rats [18]. Nevertheless, few studies have shown the expression of MFN2 in the lens and its exact role in LEC injury associated with DC.

Herein, we identified downregulated MFN2 in the lens of STZ-induced diabetic rats. Human lens epithelium HLE-B3 cells were incubated in the culture medium containing glucose at a high concentration (high glucose, HG) to induce cell injury. We unraveled the significant role of MFN2 in improving mitochondrial function, reducing apoptosis, and activating autophagy. Our findings indicate that targeting MFN2 may be a promising strategy for DC treatment.

Materials and methods

Animal model. The Ethic Committee of the China Medical University (Shenyang, China; No. cmu2022045) approved all animal experiments. Experimental procedures were carried out in accordance with relevant guidelines and regulations. In our study, healthy male SD rats were kept in a temperature- and humidity-controlled room ($22 \pm 1^\circ\text{C}$ and 45–55%, respectively) with 12 h/12 h light/dark cycle and given free access to food and water.

One week after adaptation, the rats were intraperitoneally injected with a single dose of STZ (65 mg/kg body weight) dissolved in 0.1 M sodium citrate (pH 4.5). The control rats received the vehicle only. At 72 h after STZ administration, fasting blood glucose levels were measured by a glucometer using blood taken from the tail tips. The rats with blood glucose

levels > 16.7 mM were regarded as diabetic and were selected for the following experiments. At 4, 8 and 12 weeks after STZ injection, the body weights of rats were recorded and blood was harvested from the tail tips for blood glucose level measurement. At the end of week 12, the opacity of the lens was monitored using a slit lamp [19]. All animals were euthanized via intraperitoneal (*i.p.*) injection of pentobarbital sodium overdose (200 mg/kg), and the eyeballs were excised and photographed. The lenses were then dissected and frozen at -80°C until further analyses.

Biochemical estimations. Lens tissues were immersed in saline (tissue weight (g): saline volume (mL) = 1: 10), homogenized on ice using a glass homogenizer and centrifuged at 4°C for 10 min at $8000\times g$. The supernatant was collected for quantification of protein concentration using a BCA protein quantification kit (Beyotime, Nantong, Jiangsu, China). The activity of sorbitol dehydrogenase (SDH) was estimated in accordance with the protocol of the manufacturer (Nanjing Jiancheng, Nanjing, Jiangsu, China). For measurement of lens advanced glycation end product (AGE) content, the saline was added to the lens tissues as weight (g): volume (mL) = 1: 9, and then the samples were homogenized and centrifuged at $430\times g$ for 10 min. After quantification of protein concentration (BCA kit), the AGE content was determined using an AGE detection kit (USCN, Wuhan, Hubei, China) according to the manufacturer's instruction.

Lentivirus. For overexpression, MFN2 CDS (NM_014874.3) was subcloned into a lentiviral vector pLVX-IRES-puro (FENGHUI, China). For MFN2 knockdown, short hairpin RNA (shRNA) targeting MFN2 was inserted into pLVX-shRNA1 vector (FENGHUI, China). The targeting sequence included in the shRNA was 5'-GGACGTCAAAGGTTACCTATC-3'. Lentiviruses were generated in HEK293T cells (Icellbioscience, China) transfected with plasmids pLVX-IRES-puro or pLVX-shRNA1, pSPAX2 (FENGHUI, China) and pMD2.G (FENGHUI, China) by using Lipofectamine 3000 (Invitrogen, USA) in accordance with the recommended protocols. Viral Cell supernatants containing lentiviruses were harvested after 48 h and 72 h of transfection. The transfection efficiency was measured using RT-qPCR and

western blotting assays (Fig. S1).

Cell culture and treatment. Human lens epithelial (HLE) B3 cells were obtained from American Type Culture Collection (USA) and cultured in Dulbecco's modified Eagles media (DMEM) containing 10% fetal bovine serum. The culture media were placed in an incubator at 37°C and 5% CO₂. After the cells reached 70% confluence, they were subjected to normal glucose (NG) medium (5.5 mmol/L glucose), osmolarity control medium (5.5 mmol/L glucose and 19.5 mmol/L mannitol) or high glucose (HG) medium (25 mmol/L glucose) for 48 h. NG was used as a control. In addition, prior to exposure to HG for 48 h, the cells were transfected with the above recombinant lentiviruses.

Cell counting kit-8 (CCK-8) assay. HLE-B3 cells were seeded in 96-well plates and cultured at 37°C for 48 h. Then, 10 μ L CCK-8 solution (Solarbio, Beijing, China) was added to each well, and cells were incubated for another 2 h. After that, the absorbance (optical density) was read at 450 nm with a microplate reader (800TS, Biotek, Winooski, VT, USA).

Reverse transcription quantitative polymerase chain reaction (RT-qPCR) assay. Referring to the manufacturer's instructions, total RNA from lens and HLE-B3 cells was extracted using TRIpure Isolation Reagent (BioTeke, Wuxi, Jiangsu, China) and complementary DNA (cDNA) was generated using BeyoRT II M-MLV reverse transcriptase. Then RT-qPCR reaction was done *via* SYBR Green PCR Master Mix (Solarbio). The cycling parameters were 95.00°C for 5 min and 40 cycles of 95.00°C for 10 s, 60.00°C for 10 s, 72.00°C for 15 s, followed by 72.00°C for 90 s, 40.00°C for 60 s, melting 60°C to 94°C with a 1.0°C increase every 1 s, and 25.00°C for 1–2 min. The primer sequences used were: rat MFN2 forward, 5'-GCCGTCCGTCTCATCAT-3' and reverse, 5'-GGCGGTGCAGTTCATTC-3'; homo MFN2 forward, 5'-CGCAGAAGGCTTTCAAGT-3' and reverse, 5'-ACGCATTTCCCTCGCAGTA-3'. The Ct values were recorded and the relative abundance of the products was estimated using the $2^{-\Delta\Delta Ct}$ method [20].

Mitochondrial extraction. Mitochondrial proteins were extracted using a Mitochondria Protein extraction kit (Nanjing Jiancheng). According to the manufacturer's protocols, the cells (5×10^7) were washed with phosphate-buffered saline (PBS) and centrifuged at $800\times g$, and then the cells were suspended in lysing solution for 15 min on ice. After lysing with 30–40 strokes with a homogenizer, cell supernatant was harvested by centrifugation for 5 min ($800\times g$) and transferred to a new tube. The reagents were added and the tube was centrifuged for 10 min at $15,000\times g$ at 4°C . The mitochondria (precipitate) and cytoplasm (supernatant) fractions were obtained for western blot analysis.

Western blot analysis. Total proteins were produced utilizing RIPA buffer solution (Solarbio), followed by protein concentration detection using BCA quantification kit (Solarbio). Proteins were separated by SDS-PAGE and blotted on PVDF membranes (Millipore, Burlington, MA, USA). Afterwards, the membranes were sealed with 5% (M/V) skim milk, and incubated with primary antibodies (overnight, 4°C) and secondary antibody (1 h, 37°C). The diluted antibodies used in this study contained primary antibodies against MFN2 (abclonal, A19678, 1:1000), Bcl-2 (proteintech, 12789-1-AP, 1:500), Bax (abclonal, A19684, 1:1000), cleaved caspase-9 (cst, #20750, 1:1000), Cyto c (proteintech, 10993-1-AP, 1:500), LC3II/I (abclonal, A5618, 1:1000), Beclin-1 (affinity, AF5128, 1:1000), p62 (abclonal, A19700, 1:1000), phospho (p)-mTOR (affinity, AF3308, 1:500), mTOR (affinity, AF6308, 1:500) and secondary anti-rabbit IgG, HRP-conjugated antibody (Solarbio, 1:3000). The signals were observed *via* an enhanced chemiluminescence method.

Flow cytometry analysis for cell apoptosis. To quantify apoptosis, HLE-B3 cells cultured for 48 h were harvested and incubated in the dark for 10 min with $5 \mu\text{L}$ AnnexinV-FITC and $10 \mu\text{L}$ propidium iodide (PI, Biosharp, Hefei, Anhui, China). Then, a flow cytometer (NovoCyte) was applied to analyze the percentage of apoptotic cells.

Determination of reactive oxygen species (ROS). ROS test kit was purchased from Beyotime (China). After treatment, HLE-B3 cells were incubated with diluted 2',7'-

dichlorodihydrofluorescein diacetate (DCFH-DA) reagent (1:1000) at 37°C for 20–30 min. After that, cells were collected by centrifugation for 5 min (160×g) and were resuspended in 500 μ L PBS, and then ROS was detected by flow cytometry (20000 gated cells).

Measurement of mitochondrial membrane potential ($\Delta\psi_m$). The alterations of mitochondrial membrane potential ($\Delta\psi_m$) were determined by cationic dye JC-1 (Beyotime). Cultured HLE-B3 cells were collected and stained with 1 mL JC-1 staining solution at 37°C for 20 min. After washing twice with 1× JC-1 buffer, the cells were analyzed by flow cytometry (20000 gated cells).

Data analysis. Data were expressed as mean \pm standard deviation (SD). All statistical analyses were carried out using GraphPad Prism software, version 8.0 (GraphPad Software, USA). Differences were indicated by independent sample *t*-test or one-way ANOVA, where appropriate. P values less than 0.05 were taken as statistically significant.

Results

MFN2 expression is downregulated in lens of DC rat

MFN2 has a protective effect against diabetic complications such as diabetic nephropathy; however, there is no data on whether MFN2 is implicated in DC development. In the present study, we established an *in vivo* rat model of DC *via* administrating STZ, as exhibited in Fig. 1A. Twelve weeks after STZ injection, the lenses of the rats became turbid compared with the control group (Fig. 1B). Moreover, the body weight of rats was significantly decreased at 4, 8 and 12 weeks after STZ injection. The fasting blood glucose levels were maintained above 16.7 mmol/L at 72 h after STZ induction, and increased at 4, 8 and 12 weeks after STZ injection (Fig. 1C). Besides, DC rats showed elevated SDH activity and AGE formation in the lens (Fig. 1D). Notably, RT-qPCR and western blot assays confirmed that the mRNA and protein levels of MFN2 in the lens of DC rats were significantly lower than those of control rats (Fig. 1E, F), which indicates that MFN2 may participate in DC progression.

Effect of MFN2 on morphology and viability of HLE-B3 cells

In comparison to NG group, MFN2 expression was downregulated in HLE-B3 cells treated with HG (Fig. 2A, B). To explore the effect of MFN2 on HG-induced cell injury, HLE-B3 cells were transfected with recombinant lentiviruses mediated with MFN2 overexpression plasmid (MFN2-oe) or shRNA, followed by HG induction. Then, morphological changes of HLE-B3 cells in different groups were observed under a light microscope. Under NG conditions, HLE-B3 cell morphology was regular. When exposed to HG, the cells showed elongated fibre-like form. Cell morphology turned to regular after MFN2 overexpression plasmid treatment, while cell damage appeared to be aggravated after MFN2 shRNA treatment (Fig. 2C). Besides, cell viability by CCK-8 assay was decreased after HG exposure. MFN2-oe treatment increased the viability of HLE-B3 cells, but MFN2 shRNA treatment decreased it (Fig. 2D). MFN2 protein level by western blot analysis was significantly upregulated by MFN2-oe treatment, but downregulated by MFN2 shRNA treatment (Fig. 2E).

MFN2 suppresses high glucose-induced HLE-B3 cell apoptosis

Annexin V/PI double staining assay was performed to evaluate the apoptosis of HLE-B3 cells in the presence of HG. As shown in Fig. 3A, following a 48-h treatment with HG, we observed an elevation in cell apoptosis rate. Treatment with MFN2-oe significantly reduced HG-induced HLE-B3 cell apoptosis, while MFN2 silencing increased this process. Moreover, MFN2 overexpression led to downregulated Bax and cleaved caspase-9 expression but upregulated Bcl-2 under HG conditions, and MFN2 silencing exerted the opposite effects (Fig. 3B).

MFN2 improves mitochondrial dysfunction induced by high glucose

The potential effect of MFN2 on HG-stimulated mitochondrial dysfunction in HLE-B3 cells was analyzed. ROS accumulation measured by flow cytometry was reduced following MFN2 overexpression in the presence of HG, whereas MFN2 silencing increased the ROS level (Fig. 4A). MFN2 overexpression also blunted the loss of $\Delta\psi_m$ caused by HG, while silencing MFN2 elevated it (Fig. 4B). Besides, western blot analysis showed that MFN2 overexpression declined the level of cytochrome c in the cytoplasm and increased it in the mitochondria under

HG conditions. In contrast, MFN2 silencing increased the level of Cyto c released into the cytoplasm (Fig. 4C).

MFN2 activates high glucose-induced autophagy of HLE-B3 cells

As illustrated in Fig. 5A, treatment of HLE-B3 cells with MFN2-oe increased the expression of autophagy biomarkers LC3B and Beclin-1, but decreased p62 expression under HG conditions. However, MFN2 silencing reduced LC3B and Beclin-1 levels and increased p62. Further, we paid attention to the function of MFN2 in the mTOR signaling pathway involved in cataract formation [21, 22]. Western blot analysis demonstrated that the HG-induced phosphorylation of mTOR in HLE-B3 cells was suppressed by overexpression of MFN2, whereas it was elevated by MFN2 silencing (Fig. 5B).

Discussion

In the present study, we successfully constructed a rat model of DC and demonstrated, for the first time, decreased expression of MFN2 in the lens of STZ-exposed rats, indicating that MFN2 may be a key gene associated with DC. Since the function of mRNAs in DC formation is weakly understood, our study deepened the insight on the role of MFN2 in DC. It was demonstrated that under HG conditions, *in vitro* overexpression of MFN2 could enhance cell viability, inhibit mitochondrial dysfunction and apoptosis, activate autophagy, whereas its silencing had the reverse effects. This study provides an important advance in understanding the pathogenesis of DC, and also provides a new clue for the treatment of disorders caused mainly by HG, including DC.

Lens epithelial cells (LECs) are the most active cell type in ocular lens and their abnormal function takes main blame for lens opacity. The death of LECs induced by apoptosis is a key cause of DC formation [23]. Here, we demonstrated that MFN2 was downregulated in HG-induced HLE-B3 cells. Also, MFN2 overexpression suppressed cell apoptosis, accompanied by the reduction in pro-apoptotic proteins Bax and cleaved caspase-9 and the increase in anti-apoptotic protein Bcl-2 expression. MFN2 silencing had the opposite effects. We propose that under HG conditions, MFN2 is a critical regulator of apoptosis in LECs.

There is increasing evidence that mitochondrial pathway is relevant to apoptosis and is considered to be the basic mechanism modulating cell injury [24, 25]. Previous studies have suggested that damaged mitochondria of LECs can initiate the occurrence and development of DC, and exposure of LECs to HG can result in mitochondrial dysfunction and apoptosis [26]. Consistent with these reports, in this study, increased ROS accumulation, decreased $\Delta\psi_m$ and elevated level of Cyto c released into the cytoplasm were observed, confirming the disruption of mitochondrial function in HLE-B3 cells in response to HG. MFN2, a well-known regulator of mitochondrial fusion, plays beneficial roles in diabetes-related heart diseases [27, 28]. Moreover, MFN2 deficiency has been reported to lead to abnormal mitochondrial morphology and severe mitochondrial dysfunction in mouse embryonic fibroblasts, 3T3-L1 and C2C12 cells or in macrophages [13,29,30]. In agreement with the previous reports, our study confirmed that the damage of mitochondria in HLE-B3 cells caused by HG was attenuated by treatment with MFN2-oe, but further aggravated by MFN2 silencing. On the basis of these observations, we support that MFN2 plays a key role in restoring mitochondrial function in HG-induced HLE-B3 cells. In addition, mitochondria and endoplasmic reticulum (ER) are distinct organelles that physically interact with each other, including exchange of phospholipids, calcium and other metabolites to maintain cellular integrity and bioenergetics [31–33]. Previous studies have reported that MFN2 promotes the contact of mitochondria and ER [32, 34, 35]. Whether MFN2 plays a role in mitochondria-ER contacts (MERCs) in DC deserves further investigation.

Autophagy or “self-eating” in cells is an evolutionally conserved defense and stress mechanism that exerts a critically important role in the development of diabetes as well as its complications [36, 37]. Increased or reduced autophagy may trigger cell apoptosis, and a base level of autophagy is essential for maintaining intracellular homeostasis [38, 39]. Prior studies have revealed that exposure of HLE-B3 cells to HG contributes to a low level of autophagy, thereby possibly facilitating DC formation [40], which was consistent with our observation in HLE-B3 cells. MFN2 has been reported to induce autophagy, regulate the expression of autophagy-related proteins and suppress the activation of mTOR signaling pathway in Aspc-1 cells [41]. Our current results were consistent with the previous findings, and our data

suggested that MFN2 activated autophagy in HG-treated HLE-B3 cells. Intriguingly, our results revealed that MFN2 overexpression led to a decrease in the phosphorylation of mTOR in HG-stimulated HLE-B3 cells, whereas MFN2 silencing accelerated this process, implying that mTOR signaling pathway may be one of the downstream signaling cascades implicated in MFN2-mediated regulation of autophagy. Although we demonstrated the beneficial effect of MFN2 overexpression on inhibiting HG-stimulated apoptosis, further researches are required to clarify the way MFN2 protects against HG-triggered LEC damage and to investigate whether MFN2 overexpression can alleviate the development of DC.

In summary, this report uncovers that MFN2 can inhibit mitochondrial dysfunction, elevate autophagy and reduce apoptosis in LECs cultured under HG conditions. These observations allow us to propose that MFN2 plays an important role in LECs apoptosis under HG conditions, and our study provides a new direction for DC therapy.

Article information

Data availability statement

All data used in the current study are available upon reasonable request.

Ethics statement

The Ethic Committee of the Fourth Affiliated Hospital of China Medical University (No. cmu2022045) approved all animal experiments.

Author contributions

GYG and ZJY designed the study. GYG, ZJY and LHR performed the experiments. GZ and SHY conducted the statistical analysis. GYG wrote the manuscript. All the authors have read and approved the final manuscript.

Conflict of interest

All authors claimed there was no conflict of interest.

References

1. Greenberg MJ, Bamba S. Diabetic cataracts. *Dis Mon.* 2021; 67(5): 101134, doi: [10.1016/j.disamonth.2021.101134](https://doi.org/10.1016/j.disamonth.2021.101134), indexed in Pubmed: [33485606](https://pubmed.ncbi.nlm.nih.gov/33485606/).
2. Obrosova IG, Chung SSM, Kador PF. Diabetic cataracts: mechanisms and management. *Diabetes Metab Res Rev.* 2010; 26(3): 172-180, doi: [10.1002/dmrr.1075](https://doi.org/10.1002/dmrr.1075), indexed in Pubmed: [20474067](https://pubmed.ncbi.nlm.nih.gov/20474067/).
3. Peterson SR, Silva PA, Murtha TJ, et al. Cataract Surgery in Patients with Diabetes: Management Strategies. *Semin Ophthalmol.* 2018; 33(1): 75-82, doi: [10.1080/08820538.2017.1353817](https://doi.org/10.1080/08820538.2017.1353817), indexed in Pubmed: [29144826](https://pubmed.ncbi.nlm.nih.gov/29144826/).
4. Haddad NM, Sun JK, Abujaber S, et al. Cataract surgery and its complications in diabetic patients. *Semin Ophthalmol.* 2014; 29(5-6): 329-337, doi: [10.3109/08820538.2014.959197](https://doi.org/10.3109/08820538.2014.959197), indexed in Pubmed: [25325858](https://pubmed.ncbi.nlm.nih.gov/25325858/).
5. Murtha T, Cavallerano J. The management of diabetic eye disease in the setting of cataract surgery. *Curr Opin Ophthalmol.* 2007; 18(1): 13-18, doi: [10.1097/ICU.0b013e32801129fc](https://doi.org/10.1097/ICU.0b013e32801129fc), indexed in Pubmed: [17159441](https://pubmed.ncbi.nlm.nih.gov/17159441/).
6. Long AC, Agler A, Colitz CMH, et al. Isolation and characterization of primary canine lens epithelial cells. *Vet Ophthalmol.* 2008; 11(1): 38-42, doi: [10.1111/j.1463-5224.2007.00599.x](https://doi.org/10.1111/j.1463-5224.2007.00599.x), indexed in Pubmed: [18190351](https://pubmed.ncbi.nlm.nih.gov/18190351/).
7. Su D, Hu S, Guan L, et al. Down-regulation of GJA3 is associated with lens epithelial cell apoptosis and age-related cataract. *Biochem Biophys Res Commun.* 2017; 484(1): 159-164, doi: [10.1016/j.bbrc.2017.01.050](https://doi.org/10.1016/j.bbrc.2017.01.050), indexed in Pubmed: [28088522](https://pubmed.ncbi.nlm.nih.gov/28088522/).
8. Li WC, Kuszak JR, Dunn K, et al. Lens epithelial cell apoptosis appears to be a common cellular basis for non-congenital cataract development in humans and animals. *J Cell Biol.* 1995; 130(1): 169-181, doi: [10.1083/jcb.130.1.169](https://doi.org/10.1083/jcb.130.1.169), indexed in Pubmed: [7790371](https://pubmed.ncbi.nlm.nih.gov/7790371/).
9. Li WC, Spector A. Lens epithelial cell apoptosis is an early event in the development of UVB-induced cataract. *Free Radic Biol Med.* 1996; 20(3): 301-311, doi: [10.1016/0891-5849\(96\)02050-3](https://doi.org/10.1016/0891-5849(96)02050-3), indexed in Pubmed: [8720900](https://pubmed.ncbi.nlm.nih.gov/8720900/).
10. Rovira-Llopis S, Bañuls C, Díaz-Morales N, et al. Mitochondrial dynamics in type 2 diabetes: Pathophysiological implications. *Redox Biol.* 2017; 11: 637-645, doi: [10.1016/j.redox.2017.01.013](https://doi.org/10.1016/j.redox.2017.01.013), indexed in Pubmed: [28131082](https://pubmed.ncbi.nlm.nih.gov/28131082/).
11. Delmotte P, Sieck GC. Endoplasmic reticulum stress and mitochondrial function in airway smooth muscle. *Front Cell Dev Biol.* 2019; 7: 374, doi: [10.3389/fcell.2019.00374](https://doi.org/10.3389/fcell.2019.00374), indexed in Pubmed: [32010691](https://pubmed.ncbi.nlm.nih.gov/32010691/).
12. Zorzano A, Hernández-Alvarez MI, Sebastián D, et al. Mitofusin 2 as a driver that controls energy metabolism and insulin signaling. *Antioxid Redox Signal.* 2015; 22(12): 1020-1031, doi: [10.1089/ars.2014.6208](https://doi.org/10.1089/ars.2014.6208), indexed in Pubmed: [25567790](https://pubmed.ncbi.nlm.nih.gov/25567790/).
13. Muñoz JP, Ivanova S, Sánchez-Wandelmer J, et al. Mfn2 modulates the UPR and mitochondrial function via repression of PERK. *EMBO J.* 2013; 32(17): 2348-2361, doi: [10.1038/emboj.2013.168](https://doi.org/10.1038/emboj.2013.168), indexed in Pubmed: [23921556](https://pubmed.ncbi.nlm.nih.gov/23921556/).

14. Tang WX, Wu WH, Zeng XXi, et al. Early protective effect of mitofusion 2 overexpression in STZ-induced diabetic rat kidney. *Endocrine*. 2012; 41(2): 236-247, doi: [10.1007/s12020-011-9555-1](https://doi.org/10.1007/s12020-011-9555-1), indexed in Pubmed: [22095488](https://pubmed.ncbi.nlm.nih.gov/22095488/).
15. Mi X, Tang W, Chen X, et al. Mitofusin 2 attenuates the histone acetylation at collagen IV promoter in diabetic nephropathy. *J Mol Endocrinol*. 2016; 57(4): 233-249, doi: [10.1530/JME-16-0031](https://doi.org/10.1530/JME-16-0031), indexed in Pubmed: [27997345](https://pubmed.ncbi.nlm.nih.gov/27997345/).
16. Zhang R, Garrett Q, Zhou H, et al. Upregulation of miR-195 accelerates oxidative stress-induced retinal endothelial cell injury by targeting mitofusin 2 in diabetic rats. *Mol Cell Endocrinol*. 2017; 452: 33-43, doi: [10.1016/j.mce.2017.05.009](https://doi.org/10.1016/j.mce.2017.05.009), indexed in Pubmed: [28487236](https://pubmed.ncbi.nlm.nih.gov/28487236/).
17. Zhao J, Wu X, Wu D, et al. Embryonic surface ectoderm-specific mitofusin 2 conditional knockout induces congenital cataracts in mice. *Sci Rep*. 2018; 8(1): 1522, doi: [10.1038/s41598-018-19849-2](https://doi.org/10.1038/s41598-018-19849-2), indexed in Pubmed: [29367651](https://pubmed.ncbi.nlm.nih.gov/29367651/).
18. Yang J, Wang T, Zhang Y, et al. Altered expression of mitofusin 2 in penile tissues of diabetic rats. *Andrologia*. 2014; 46(5): 522-528, doi: [10.1111/and.12108](https://doi.org/10.1111/and.12108), indexed in Pubmed: [23682852](https://pubmed.ncbi.nlm.nih.gov/23682852/).
19. Bahmani F, Bathaie SZ, Aldavood SJ, et al. Prevention of α -crystallin glycation and aggregation using l-lysine results in the inhibition of in vitro catalase heat-induced-aggregation and suppression of cataract formation in the diabetic rat. *Int J Biol Macromol*. 2019; 132: 1200-1207, doi: [10.1016/j.ijbiomac.2019.04.037](https://doi.org/10.1016/j.ijbiomac.2019.04.037), indexed in Pubmed: [30965074](https://pubmed.ncbi.nlm.nih.gov/30965074/).
20. Zhao F, Maren NA, Kosentka PZ, et al. An optimized protocol for stepwise optimization of real-time RT-PCR analysis. *Hortic Res*. 2021; 8(1): 179-332, doi: [10.1038/s41438-021-00616-w](https://doi.org/10.1038/s41438-021-00616-w), indexed in Pubmed: [34333545](https://pubmed.ncbi.nlm.nih.gov/34333545/).
21. He L, Zhang N, Wang L, et al. Quercetin inhibits AQP1 translocation in high-glucose-cultured SRA01/04 cells through PI3K/AKT/mTOR pathway. *Curr Mol Pharmacol*. 2021; 14(4): 587-596, doi: [10.2174/1874467213666200908120501](https://doi.org/10.2174/1874467213666200908120501), indexed in Pubmed: [32900356](https://pubmed.ncbi.nlm.nih.gov/32900356/).
22. Li J, Sun Q, Qiu X, et al. Downregulation of AMPK dependent FOXO3 and TFEB involves in the inhibition of autophagy in diabetic cataract. *Curr Eye Res*. 2022; 47(4): 555-564, doi: [10.1080/02713683.2021.2009516](https://doi.org/10.1080/02713683.2021.2009516), indexed in Pubmed: [34872443](https://pubmed.ncbi.nlm.nih.gov/34872443/).
23. Kim J, Kim CS, Sohn E, et al. Lens epithelial cell apoptosis initiates diabetic cataractogenesis in the Zucker diabetic fatty rat. *Graefes Arch Clin Exp Ophthalmol*. 2010; 248(6): 811-818, doi: [10.1007/s00417-010-1313-1](https://doi.org/10.1007/s00417-010-1313-1), indexed in Pubmed: [20162295](https://pubmed.ncbi.nlm.nih.gov/20162295/).
24. Babizhayev MA, Yegorov YE. Reactive oxygen species and the aging eye: specific role of metabolically active mitochondria in maintaining lens function and in the initiation of the oxidation-induced maturity onset cataract--a novel platform of mitochondria-targeted antioxidants with broad therapeutic potential for redox regulation and detoxification of oxidants in eye diseases. *Am J Ther*. 2016; 23(1): e98-117, doi: [10.1097/MJT.0b013e3181ea31ff](https://doi.org/10.1097/MJT.0b013e3181ea31ff), indexed in Pubmed: [21048433](https://pubmed.ncbi.nlm.nih.gov/21048433/).

25. Yao Ke, Ye P, Zhang Li, et al. Epigallocatechin gallate protects against oxidative stress-induced mitochondria-dependent apoptosis in human lens epithelial cells. *Mol Vis.* 2008; 14: 217–223, indexed in Pubmed: [18334937](#).
26. Li Yi, Jia Yi, Zhou J, et al. Effect of methionine sulfoxide reductase B1 silencing on high-glucose-induced apoptosis of human lens epithelial cells. *Life Sci.* 2013; 92(3): 193–201, doi: [10.1016/j.lfs.2012.11.021](#), indexed in Pubmed: [23270945](#).
27. Yu H, Hong X, Liu L, et al. Cordycepin decreases ischemia/reperfusion injury in diabetic hearts via upregulating ampk/mfn2-dependent mitochondrial fusion. *Front Pharmacol.* 2021; 12: 754005, doi: [10.3389/fphar.2021.754005](#), indexed in Pubmed: [34744731](#).
28. Hu L, Ding M, Tang D, et al. Targeting mitochondrial dynamics by regulating Mfn2 for therapeutic intervention in diabetic cardiomyopathy. *Theranostics.* 2019; 9(13): 3687–3706, doi: [10.7150/thno.33684](#), indexed in Pubmed: [31281507](#).
29. Hu Y, Chen H, Zhang L, et al. The AMPK-MFN2 axis regulates MAM dynamics and autophagy induced by energy stresses. *Autophagy.* 2021; 17(5): 1142–1156, doi: [10.1080/15548627.2020.1749490](#), indexed in Pubmed: [32249716](#).
30. Tur J, Pereira-Lopes S, Vico T, et al. Mitofusin 2 in macrophages links mitochondrial ROS production, cytokine release, phagocytosis, autophagy, and bactericidal activity. *Cell Rep.* 2020; 32(8): 108079, doi: [10.1016/j.celrep.2020.108079](#), indexed in Pubmed: [32846136](#).
31. Arruda AP, Hotamisligil GS, Fu S, et al. Phenotypic assays identify azoramidate as a small-molecule modulator of the unfolded protein response with antidiabetic activity. *Sci Transl Med.* 2015; 7(292): 292ra98–397, doi: [10.1126/scitranslmed.aaa9134](#), indexed in Pubmed: [26084805](#).
32. Naón D, Hernández-Alvarez MI, Shinjo S, et al. Genes involved in mitochondrial biogenesis/function are induced in response to bilio-pancreatic diversion in morbidly obese individuals with normal glucose tolerance but not in type 2 diabetic patients. *Diabetologia.* 2009; 52(8): 1618–1627, doi: [10.1007/s00125-009-1403-y](#), indexed in Pubmed: [19504086](#).
33. Ding Y, Liu N, Zhang D, et al. Mitochondria-associated endoplasmic reticulum membranes as a therapeutic target for cardiovascular diseases. *Front Pharmacol.* 2024; 15: 1398381, doi: [10.3389/fphar.2024.1398381](#), indexed in Pubmed: [38694924](#).
34. de Brito O, Scorrano L. Mitofusin 2 tethers endoplasmic reticulum to mitochondria. *Nature.* 2008; 456: 605–610.
35. Cao Y, Chen Z, Hu J, et al. Mfn2 regulates high glucose-induced mams dysfunction and apoptosis in podocytes via PERK pathway. *Front Cell Dev Biol.* 2021; 9: 769213, doi: [10.3389/fcell.2021.769213](#), indexed in Pubmed: [34988075](#).

36. Barlow AD, Thomas DC. Autophagy in diabetes: β -cell dysfunction, insulin resistance, and complications. *DNA Cell Biol.* 2015; 34(4): 252–260, doi: [10.1089/dna.2014.2755](https://doi.org/10.1089/dna.2014.2755), indexed in Pubmed: [25665094](https://pubmed.ncbi.nlm.nih.gov/25665094/).
37. Tao T, Xu H. Autophagy and obesity and diabetes. *Adv Exp Med Biol.* 2020; 1207: 445–461, doi: [10.1007/978-981-15-4272-5_32](https://doi.org/10.1007/978-981-15-4272-5_32), indexed in Pubmed: [32671767](https://pubmed.ncbi.nlm.nih.gov/32671767/).
38. Clarke PGH, Puyal J. Autophagic cell death exists. *Autophagy.* 2012; 8(6): 867–869, doi: [10.4161/auto.20380](https://doi.org/10.4161/auto.20380), indexed in Pubmed: [22652592](https://pubmed.ncbi.nlm.nih.gov/22652592/).
39. Fitzwalter BE, Thorburn A. Recent insights into cell death and autophagy. *FEBS J.* 2015; 282(22): 4279–4288, doi: [10.1111/febs.13515](https://doi.org/10.1111/febs.13515), indexed in Pubmed: [26367268](https://pubmed.ncbi.nlm.nih.gov/26367268/).
40. Li Ji, Ye W, Xu W, et al. Activation of autophagy inhibits epithelial to mesenchymal transition process of human lens epithelial cells induced by high glucose conditions. *Cell Signal.* 2020; 75: 109768, doi: [10.1016/j.cellsig.2020.109768](https://doi.org/10.1016/j.cellsig.2020.109768), indexed in Pubmed: [32896607](https://pubmed.ncbi.nlm.nih.gov/32896607/).
41. Xue R, Meng Q, Lu Di, et al. Mitofusin2 induces cell autophagy of pancreatic cancer through inhibiting the PI3K/AKT/mTOR signaling pathway. *Oxid Med Cell Longev.* 2018; 2018: 2798070, doi: [10.1155/2018/2798070](https://doi.org/10.1155/2018/2798070), indexed in Pubmed: [30046371](https://pubmed.ncbi.nlm.nih.gov/30046371/).

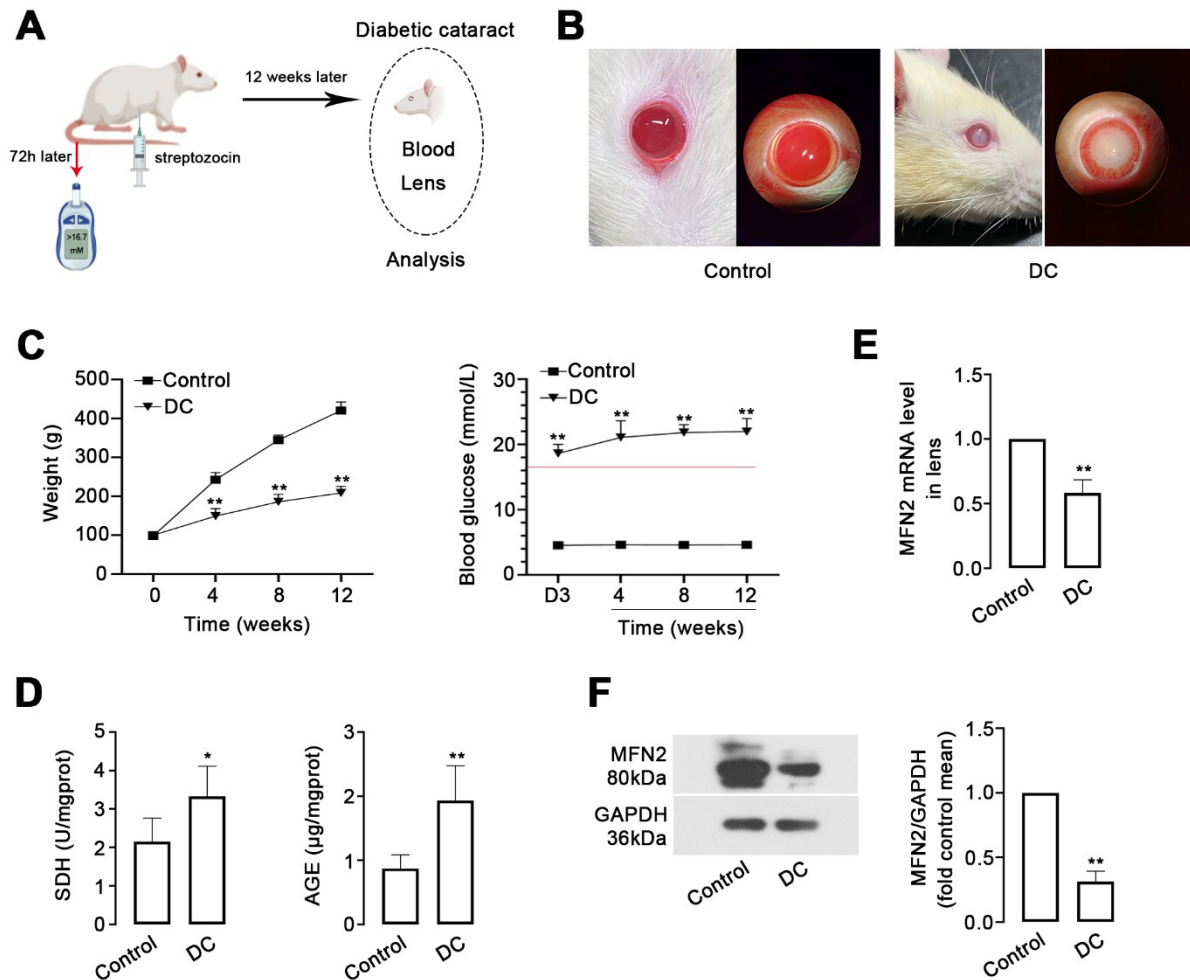


Figure 1. MFN2 involved in diabetic cataract formation. **A.** Experimental design. Healthy male SD rats were subjected to 65 mg/kg streptozocin (STZ) intraperitoneally. After 72 h, the fasting blood glucose was evaluated. Rats with blood glucose levels greater than 16 mM were selected for further study. **B.** After 12 weeks, representative slit lamp photographs of lens were shown. **C.** The average body weight of diabetic rats and average blood glucose level at different time points after STZ injection. **D.** Changes in SDH and AGE levels in lens. **E, F.** MFN2 expression was downregulated in the lens of rats with diabetic cataract as displayed by RT-qPCR and western blot. *P < 0.05, **P < 0.01 vs. the control.

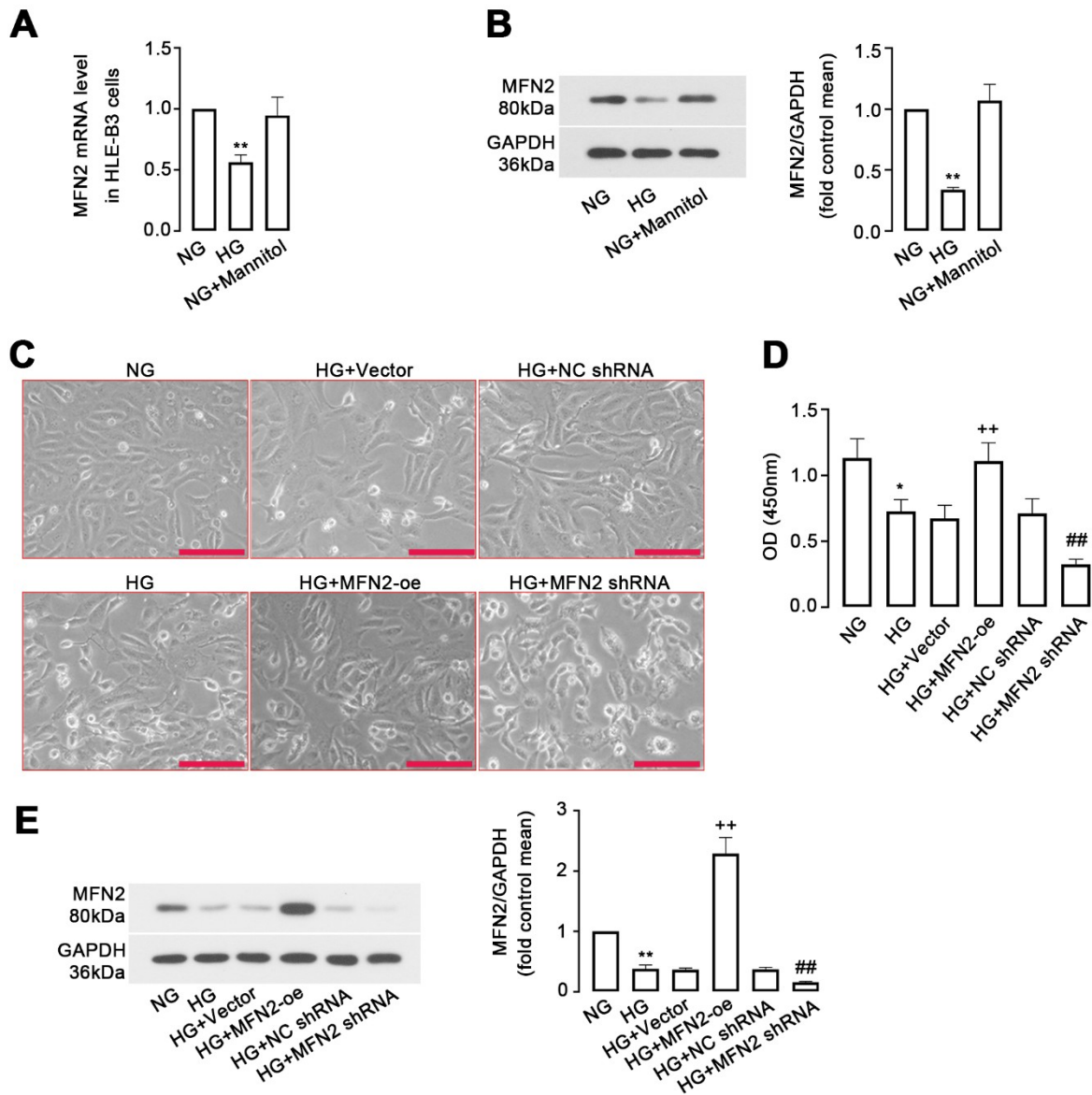


Figure 2. MFN2 expression in high glucose-induced HLE-B3 cells. **A, B.** HLE-B3 cells were treated with high glucose (HG), normal glucose (NG), or mannitol for 48 h, and then MFN2 expression was confirmed by RT-qPCR and western blot assays. **C.** HLE-B3 cells were transfected with lentivirus-mediated MFN2 overexpression vector or shRNA for 48 h, followed by HG or NG treatment for another 48 h. The morphological change of HLE-B3 cells was shown. Black arrows point to individual cells. Scale bar = 200 μm. **D.** CCK-8 assay revealed cell viability in different groups. **E.** The protein level of MFN2 in HLE-B3 cells, as measured by western blot. * $P < 0.05$, ** $P < 0.01$, NG as control; ** $P < 0.01$, HG+Vector as control; ## $P < 0.01$, HG + NC shRNA as control.

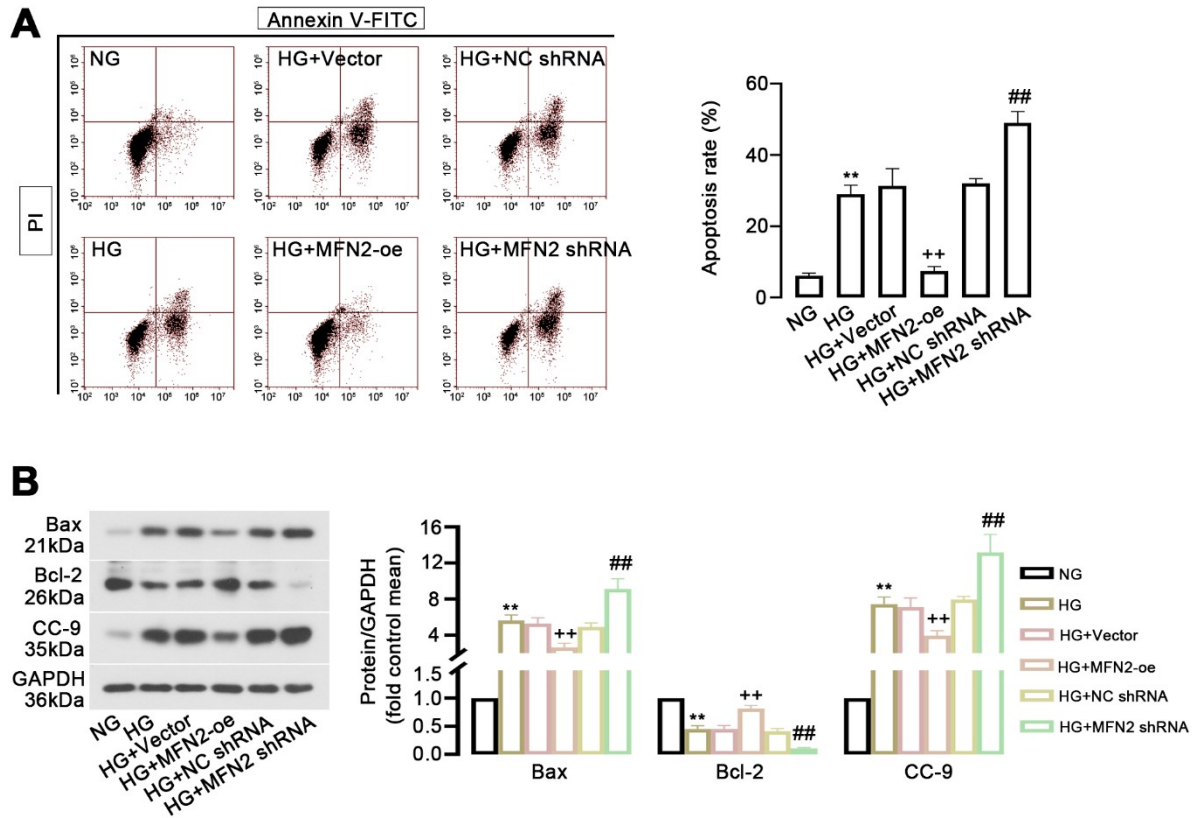


Figure 3. MFN2 regulates HLE-B3 cell apoptosis in response to HG. **A.** Flow cytometry was performed to measure the apoptosis rate of HLE-B3 cells in response to HG. **B.** Western blot characterization of apoptosis-related proteins and quantification. ** $P < 0.01$, NG as control; + $P < 0.01$, HG + Vector as control; ## $P < 0.01$, HG + NC shRNA as control.

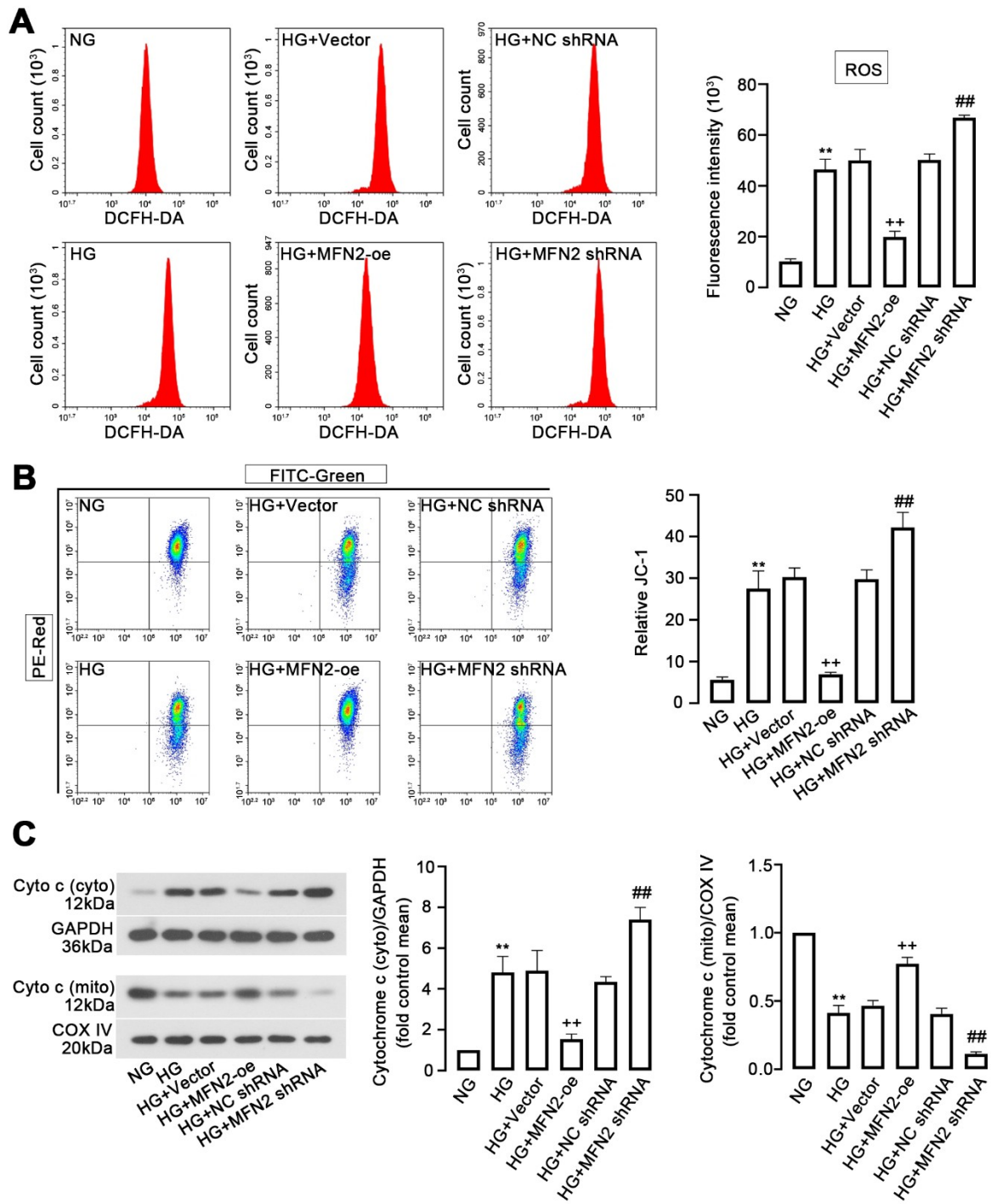


Figure 4. MFN2 affects mitochondria damage in HLE-B3 cells under HG conditions. **A.** Flow cytometry showed ROS level in HLE-B3 cells. **B.** Analysis of mitochondrial membrane potential by JC-1. **C.** Cytochrome c (Cyto c) expression in cytoplasm and mitochondria. **P < 0.01, NG as control; **P < 0.01, HG+Vector as control; ##P < 0.01, HG + NC shRNA as control.

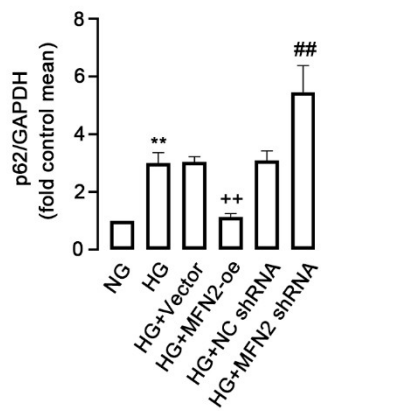
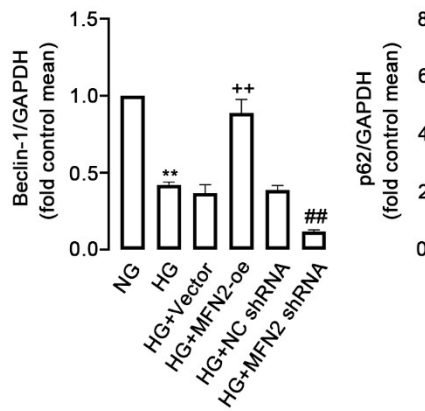
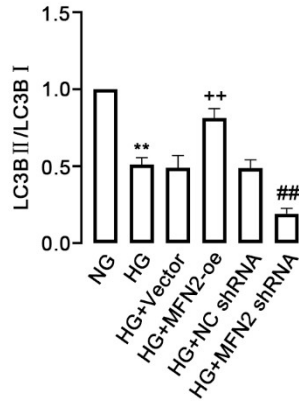
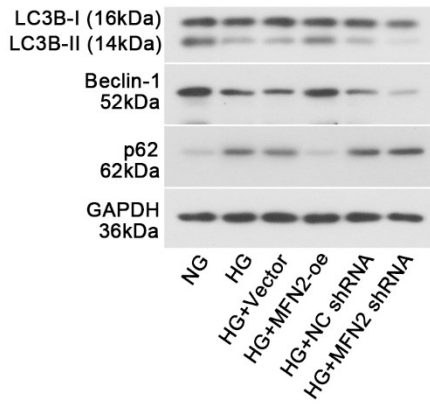
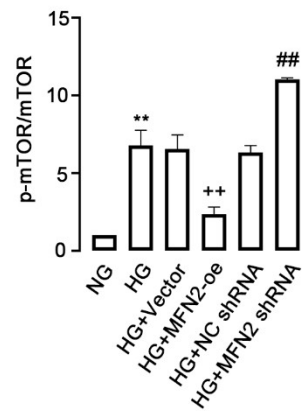
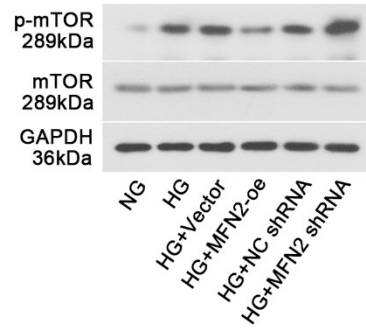
A**B**

Figure 5. MFN2 alters autophagy in HLE-B3 cells upon HG stress. **A.** Western blot analysis of the markers (LC3BII, LC3BI, Beclin-1, p62) of autophagy in HLE-B3 cells. **B.** Western blot analysis of mTOR pathway-related proteins. **P < 0.01, NG as control; ++P < 0.01, HG + Vector as control; ##P < 0.01, HG + NC shRNA as control.

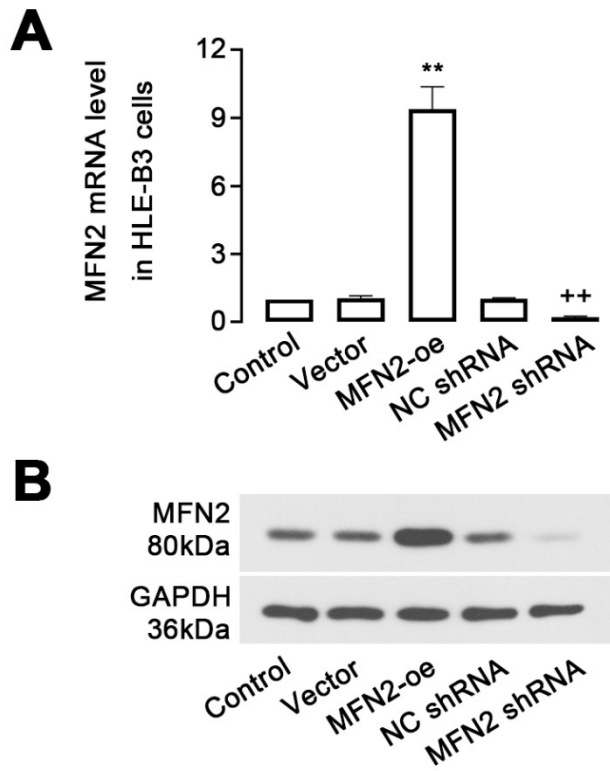


Figure S1. MFN2 expression in HLE-B3 cells overexpressing or knocking down MFN2. **A,** **B.** HLE-B3 cells were transfected with lentivirus-mediated MFN2 overexpression vector or shRNA for 48 h, and RT-qPCR and western blot assays were performed to detect the MFN2 expression level as described in Methods section.